Microchimica Acta (2022) 189: 327
https://doi.org/10.1007/s00604-022-05431-1

ORIGINAL PAPER

Silver-manganese nanocomposite modified screen-printed carbon electrode in the fabrication of an electrochemical, disposable biosensor strip for cystic fibrosis

P. Arun Kumar[1,2] · Aarathi Pradeep[1,2] · Bipin Kumar G. Nair[1,3,4] · T. G. Satheesh Babu[1,2,4] · Punathil Vasu Suneesh[1,2]

Received: 29 March 2022 / Accepted: 25 July 2022 / Published online: 11 August 2022

Abstract

A silver-manganese nanocomposite was successfully prepared by the urea hydrolysis method and used to detect chloride ions in sweat electrochemically. The synthesis involves the reaction of manganese sulphate, silver nitrate, and urea at 100 °C for 24 h. The crystalline nature of the particle was studied by diffraction analysis and found to be mixed-phase oxides of manganese alongside the oxides of silver. Morphological studies revealed the presence of quasi-prism-like structures, which is characteristic of β-MnO_2. A disposable sensor was fabricated by screen-printing the catalyst and used for the electrochemical detection of chloride ions in sweat. The sensor exhibited good selectivity, a sensitivity of 22.93 ± 0.64 μA mM^{-1} cm^{-2} in solution and 3010 ± 60 μA (log mM) $^{-1}$ cm^{-2} for the fabricated sensor strip with a detection range from 5 mM up to 200 mM. The detection limit is 207 ± 7 μM (S/N = 3) in solution and 17 ± 6 μM for the fabricated sensor strip. The relative standard deviation (RSD) of sensor response is 2.38%. A prototype of the biosensor strip was fabricated and validated using real samples. This brings the possibility of developing a real-time biosensor strip for cystic fibrosis in point-of-care testing applications.

Keywords Silver-manganese nanocomposite · Screen printing · Electrochemical chloride sensor · Biosensor strip · Sweat chloride · Cystic fibrosis

Introduction

Cystic Fibrosis (CF) is an autosomal dormant and innate genetic disorder that affects several organs, including the lungs, pancreas, intestine, liver, and reproductive system. Early diagnosis of CF helps in better treatment and control. Newborn screening for CF can reduce hospitalizations, minimize the symptoms, achieve nutritional benefits, and potentially better lung function [1]. Mutation in a gene responsible for coding the protein CF Transmembrane Conductance Regulator causes abnormality leading to CF. The transfigured gene involves the production of abnormal, sticky mucus, which clogs the ductules and thereby causes infection and organ system damage. This also affects the reabsorption of electrolytes in duct epithelium. Testing of chloride ion imbalance in sweat is the gold standard for diagnosing CF. In patients diagnosed with CF, the sweat contains a higher level of chloride ions, typically 60–150 mM. But for a healthy individual, the sweat chloride value is below 40 mM [1, 2]. The CF diagnosis by sweat chloride determination involves the collection of a sweat sample followed by quantification by coulometric titration, manual titration, flame photometry, optical methods, or using an ion-selective electrode [1, 2].

Different techniques are employed to determine chloride ions based on the charge on the electrode surface and the mass transfer mechanism. Potentiometric detection of chloride ions using silver screen-printed electrodes (SPE) for sensing and pilocarpine for sweat generation was capable

✉ Punathil Vasu Suneesh
pv_suneesh@cb.amrita.edu

1 Amrita Biosensor Research Lab, Amrita School of Engineering, Amrita Vishwa Vidyapeetham, Coimbatore, India

2 Department of Sciences, Amrita School of Physical Sciences, Amrita Vishwa Vidyapeetham, Coimbatore, India

3 Amrita School of Biotechnology, Amrita Vishwa Vidyapeetham, Amritapuri, India

4 Amrita Biomedical Engineering Centre, Amrita School of Engineering, Amrita Vishwa Vidyapeetham, Coimbatore, India

of quantifying chloride ions directly on the skin [3]. Carbon paste electrodes modified with silver nanoparticles are also used in the voltammetric determination of chloride ions. Advantages of this method include its portability and adaptability [4]. SPE modified with silver nanoparticles was used for the oxidative stripping voltammetric analysis of different concentrations of chloride ions. Sensor electrodes were tested with synthetic sweat samples and spiked sweat to establish the possibility for real-time application of the fabricated sensor [5]. Other SPE-based voltammetric sensors have been used to determine chloride ions in different samples, including saline and ocean waters, and some are fabricated as wearable chloride ion sensors [6, 7].

Catalysts including silver nanoparticles, multiwalled carbon nanotubes modified with copper benzene-1,3,5 tricarboxylate on polytetrafluoroethylene substrate [8], indium-gallium tin oxide modified with graphene oxide [9], and platinum-based SPE [10] are also reported for electrochemical detection of chloride ions. Ion-selective electrodes (ISE), which measure the potential difference between two sides of an ionophore membrane, are commonly used to detect chloride ions [11]. The effectiveness of detection depends directly on the ionophores. Some widely reported ionophore membrane components include modified crown ether, tridodecyl methylammonium chloride, and ETH ionophores series. Ionophores like tripodal squaramide derivative [12] and composites like modified polypyrrole/graphite-epoxy [11] are synthesized explicitly for the potentiometric testing of chloride ions in biological fluids [13]. Besides potentiometric sensors, field-effect transistors (FET) are fabricated for chloride ion detection. The electrode consists of polycrystalline diamond whose surface was modified with hydrogen terminals. The shift in voltages of FET caused by the concentration of chloride or bromide ions is quantified [14].

Other types of chloride sensors include integrated Ag/AgCl electrodes with high electron mobility transistors [15], Ag/AgCl electrodes for chronopotentiometric testing in concrete structures [16], and underpotential deposited Ag layer on nanoporous gold electrode surface [17]. Silver-modified SPE is used for environmental chloride sensing in soil samples [18]. A metal–organic framework modified with silver nanoparticles was used for voltammetric sensing of serum chloride [19]. Nanoparticles of α-MnO_2-CO_3O_4 were used in the fabrication of chloride sensors. The solvothermal synthesis gives the nanomaterial a controlled structure responsible for their improved chloride sensing characteristics. Thus, semiconductor nanomaterials doped with transition metals like manganese show high potential in sensing applications [20].

Oxides of manganese exhibit high mechanical flexibility, low intrinsic electrical conductivity, and excellent stability. They can be synthesized in different shapes and sizes, each with unique surface morphology, electron rate transfer, and readiness for modification [21]. Manganese-based nanocomposites are also utilized to detect various biomarkers, including hydrogen peroxide, cholesterol, ascorbic acid, uric acid, dopamine, and glutathione. The synergistic effect of materials like silver nanoparticles with oxides of manganese results in excellent conductivity due to a high electron transfer rate and great catalytic performances [21–23]. This suggests the utilization of a silver-manganese composite for sensing chloride ions.

There are attempts to fabricate biosensors as disposable test strips or chips for self-monitoring. Our previous work attempts to develop a disposable biosensor strip for the amperometric detection of whole blood glucose by screen printing electrodes and integrating electrolyte membrane [24]. A tiny, flexible, wireless, integrated system was fabricated utilizing flexible circuitry and screen-printed electrodes for potentiometric determination of pH and amperometric determination of chloride ions [25]. Another flexible electrochemical system was developed for electrochemical determination of calcium and chloride ions in body fluids by screen printing stretchable circuitry, integrating with microfluidics and smartphone interface [26]. A biosensor for CF monitoring was built by integrating a system for sweat collection and an array of solid-state potentiometric microsensors to analyze specific markers. Sensor arrays with an ion-selective type of electrodes were connected to a flow cell and a portable analytical instrumentation system. Monitoring CF by this method showed good response and stability. However, the interference from nitrate ions is a setback [27]. A wearable sensor typically employs pilocarpine-induced iontophoresis for sweat generation and a macroduct sweat collection system. The main advantage of this method of sweat chloride monitoring includes rapid results and the requirement of low sample volume, which is desirable in the case of screening infants [28]. A paper-based SPE was reported, prepared with silver electrodes for chloride ion sensing in serum and sweat samples using voltammetric analysis. The main advantage is that they are disposable, easy to use, and require only a small sample volume [29].

The present work utilizes silver-manganese nanocomposite for the selective and sensitive electrochemical sensing of chloride ions. A biosensor test strip was fabricated by screen printing and assembling different layers of membranes. The membranes are responsible for the storage of electrolytes and the smooth flow of the sample fluid. Sweat samples collected from individuals were used to test the real-time application of the fabricated disposable sensor strip. The ease of fabrication combined with good selectivity and sensitivity invites the possibility for this biosensor strip to be integrated into a Point-of-Care-Testing (PoCT) device for the diagnosis of cystic fibrosis.

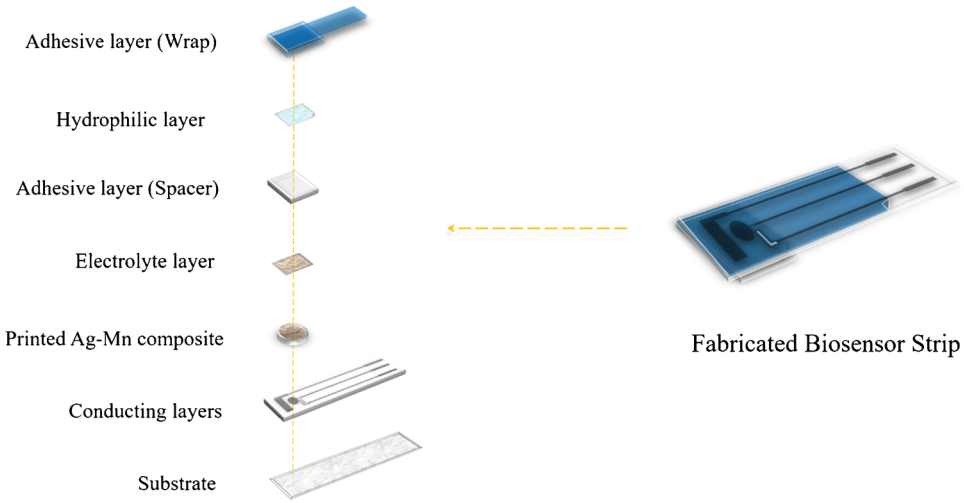

Scheme1 Components of biosensor test strip for the detection of chloride ions in body fluids

Materials and methods

Reagents and instruments

D(+)Glucose (≥99.5%), L-ascorbic acid (>99%), dopamine hydrochloride (≥98.5%), uric acid (≥99%), creatinine (≥98%), lactose (>98%), alanine (>98%), aspartic acid (>98%), and glycine (≥99% pure) were purchased from Sigma-Aldrich (https://www.sigmaaldrich.com/india.html). Silver nitrate, sodium sulphate, sodium phosphate, sodium bicarbonate, manganese sulphate, urea, barium chloride, sodium chloride, sodium nitrate, and common salts of analytical grades were purchased from Finar Ltd (https://www.finarchemicals.com/). Centrifuge tubes and vials used were purchased from Tarsons (https://www.tarsons.com/). Millipore water (15.2 MΩ cm) was used for catalyst synthesis, preparation of reagents, and washing.

A benchtop centrifuge (5810R, Eppendorf, Germany) was used for washing and extracting the compound from the reaction mixture. A semi-automated screen printer (TP-450 SL Hanky, Taiwan) was used to fabricate printed sensor electrodes. An electrochemical workstation (CHI660C, CH Instruments, USA) was used for all the electrochemical analyses. FESEM (SIGMA VP, ZEISS, Germany), and HRTEM (JEM 2100, Joel Ltd, Japan) were used for morphological characterization, and X-Ray Powder Diffractometer (AXS D8 Advance, Bruker, USA) for the crystalline characterization of compounds. The Millipore water used in the study was obtained from Millipore—Elix 10 system (Millipore, Germany).

Synthesis of catalyst

The catalyst was prepared by heating 37.5 mM of silver nitrate, 37.5 mM of manganese sulphate, and 750 mM of urea in a rota mantle for 24 h at 100 °C under constant stirring. After completion of the reaction, the solid mass formed was washed with Millipore water till the catalyst was free of nitrate and sulphate ion impurities. This compound was dried to form a brownish compound and labelled as Ag-Mn. Similarly, to understand the effect of Ag and Mn in the catalyst, different samples were prepared by varying the mole ratio of the precursors, as mentioned in the supplementary Table S1.

Fabrication of a biosensor test strip

The prepared catalysts were printed onto the working area of screen-printed carbon electrodes (SPE) to fabricate the sensor. SPE was fabricated following the same procedure discussed in our previous works [24, 30]. The catalytic ink was made by mixing 400 mg of catalyst and 600 mg of carbon ink, screen printed, and dried at 80 °C for 10 min. The printed electrodes were fabricated as a biosensor strip prototype for testing chloride ions in real-time. First, a cellulose membrane was treated with 2 M sodium nitrate, dried, and used as an electrolyte reservoir. This electrolyte layer was covered by an adhesive spacer layer followed by a hydrophilic membrane. The electrolyte and hydrophilic membranes were uniformly sheared to ensure high uniformity and repeatability. Adhesive layers were defined by laser cutting, so the errors associated with manual procedures could be minimized. An adhesive wrap is finally used to cover all the layers and bind them together. The designated sample space ensures that an equal sample volume enters every sensor and confirms equal dilution of the solid electrolyte, leading to enhanced repeatability in measurements. The components of the sensor strip are shown in Scheme 1.

Real sample analysis

The fabricated sensor was initially tested against a simulated sweat solution to calibrate the test strip. To prepare simulated sweat, Millipore water was initially warmed up to 38 ℃ to match human skin temperature, followed by the addition of 58.3 mg L^{-1} sodium sulphate, 252 mg L^{-1} sodium bicarbonate, 48.4 mg L^{-1} sodium phosphate, 30.6 mg L^{-1} D(+)glucose, 51.1 mg L^{-1} D(+)alanine, 45.3 mg L^{-1} aspartic acid, 29.3 mg L^{-1} glycine, 9.92 mg L^{-1} uric acid, 601 mg L^{-1} urea, 9.5 mg L^{-1} creatinine and 1.76 mg L^{-1} ascorbic acid [33]. The pH was adjusted to 5.5 with the help of 1 M sulphuric acid. The strip was calibrated using simulated sweat with different concentrations of chloride ions.

For real-time application, the fabricated sensor strip is tested against body sweat extracted during a treadmill run from healthy individuals. As electrolyte and hydrophilic membranes were integrated with the SPE using adhesive layers, no other electrolyte or reagents were required during the testing. The user only needs to introduce about 20 µL of sweat sample without any preprocessing. With the assistance of intricate designs made in adhesive layers, the sweat sample flows through the layers of the sensor strip and gets collected in the working area. The measurements are carried out using Differential pulse voltammetry (DPV) under a potential window of − 0.25 V to + 0.25 V, with an increment potential of 1 mV, a pulse width of 0.06 s, and a pulse amplitude of 25 mV.

Results and discussion

Morphological characterization

The size and morphology of Ag-Mn were studied using FESEM. Different shapes of the sample were recorded at higher and lower magnification (Fig. 1A–C). The obtained micrographs showed the presence of a uniform arrangement of well-defined nanorods with lengths ranging from 100 to 1000 nm and widths from 50 to 200 nm. The presence of silver and manganese along with oxygen is evident from SEM–EDX analysis (Table S2). The prepared sample consists only of silver and manganese in oxide form, as no other peaks (impurities) could be observed. TEM analysis showed a defined quasi-prism structure of individual nanorods in the prepared sample (Fig. 1D–F). This structure is attributed to the presence of β-phase manganese oxide [31]. Adopting the urea hydrolysis method for synthesis contributed to the controlled synthesis of the catalyst with a defined structure. The presence of multiple planes corresponding to β-MnO_2, oxides of manganese, and Ag NPs was calculated from the SAED pattern, which is also supported by XRD patterns.

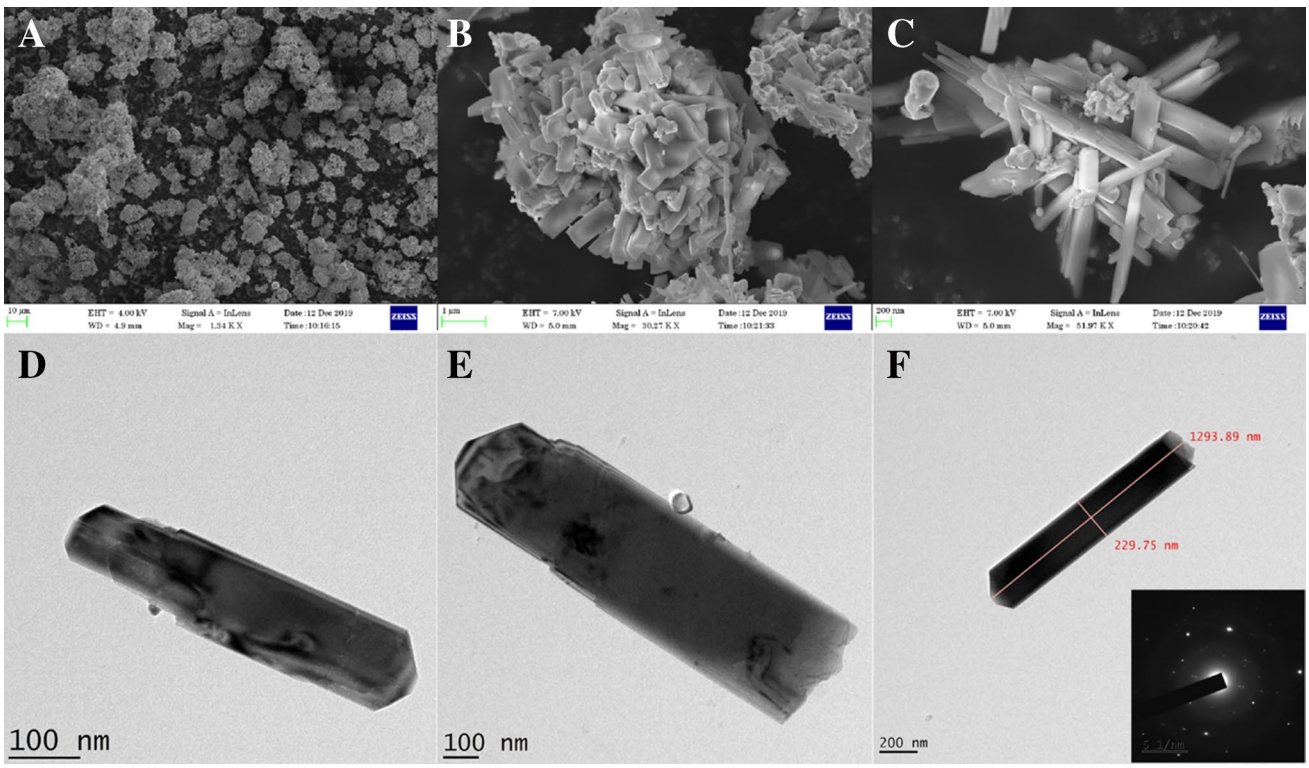

Fig. 1 FESEM images of Ag-Mn composite recorded at low (**A**, **B**) and high magnification (**C**), HRTEM images of Ag-Mn composite showing quasi-prism structure (**D**, **E**) and dimensions of the nanorods (**F**), F-inset: SAED pattern

The presence of additional peaks in SAED and identified planes in XRD (Fig. S1) suggests the existence of manganese in different oxidation states, i.e., mixed-phase manganese oxide along with silver nanoparticles.

Electrochemical characterization

The electrochemical characterization of SPE was carried out in a sodium nitrate medium over a potential range from 0 to 0.4 V with a scan rate of 50 mV s^{-1}. No characteristic peaks were observed when the electrode was analyzed in the absence of chloride ions. In the presence of chloride ions, a redox peak was observed near 0.1 V. The peak current was found to increase linearly upon increasing chloride ion concentration with a negative shift in potential.

Electrochemical detection of chloride ions

Sensor electrodes were fabricated with different compositions of catalysts, as mentioned in Table S1. They were tested using linear sweep voltammetry in 0.1 M sodium nitrate medium with 100 mM NaCl (Fig. 2A). The bare SPE shows a negligible response towards chloride ions, and the electrode fabricated with sample-Mn shows a feeble response, and the presence of silver in the composite enhances the electrocatalytic activity. The electrode fabricated with Ag-Mn showed the maximum response; hence all further analyses were carried out with this electrode. The effect of scan rate on the electrooxidation of silver and the formation of silver chloride was studied in a solution containing 0.1 M $NaNO_3$ and 5 mM NaCl at a potential range from 0 to + 0.2 V (Fig. 2B). A plot of the square root of the scan rate against the peak current follows a linear behaviour (inset, Fig. 2B). This establishes that the electron transfer reaction in the presence of chloride ions is diffusion controlled.

An electrochemical study (DPV) of the fabricated electrode in the presence of chloride ions showed a defined peak near 0.05 V. This peak can be attributed to the conversion of silver present in the silver-manganese electrode material to silver chloride. This is further confirmed by testing a silver ink-coated electrode in the same conditions. The oxidation peaks in both cases were observed at a potential near 0.05 V with a similar magnitude of the current.

$$Ag + Cl^- \rightarrow AgCl + e^- \quad (1)$$

A peak at the lower potential range suggests the easy formation of silver chloride, as established by Toh et al. [5]. With an increase in chloride level in the test solution, an increase in this peak current was also observed. Hence, this peak height correlates with the concentration and is used to quantify chloride ions. EDS and SEM analysis of the Ag-Mn/SPE was carried out before and after testing with chloride solutions to support the sensor's working mechanism. The SEM images of the Ag-Mn/SPE (Fig. S3A), tested in sodium nitrate medium (Fig. S3B) and sodium nitrate-containing sodium chloride (Fig. S3C), along with their elemental mapping (Fig. S4), shows a higher percentage of silver chloride on the electrode after testing in a solution containing chloride. The enhanced proportion of silver chloride on Ag-Mn/SPE is attributed to the conversion of Ag into AgCl. This study,

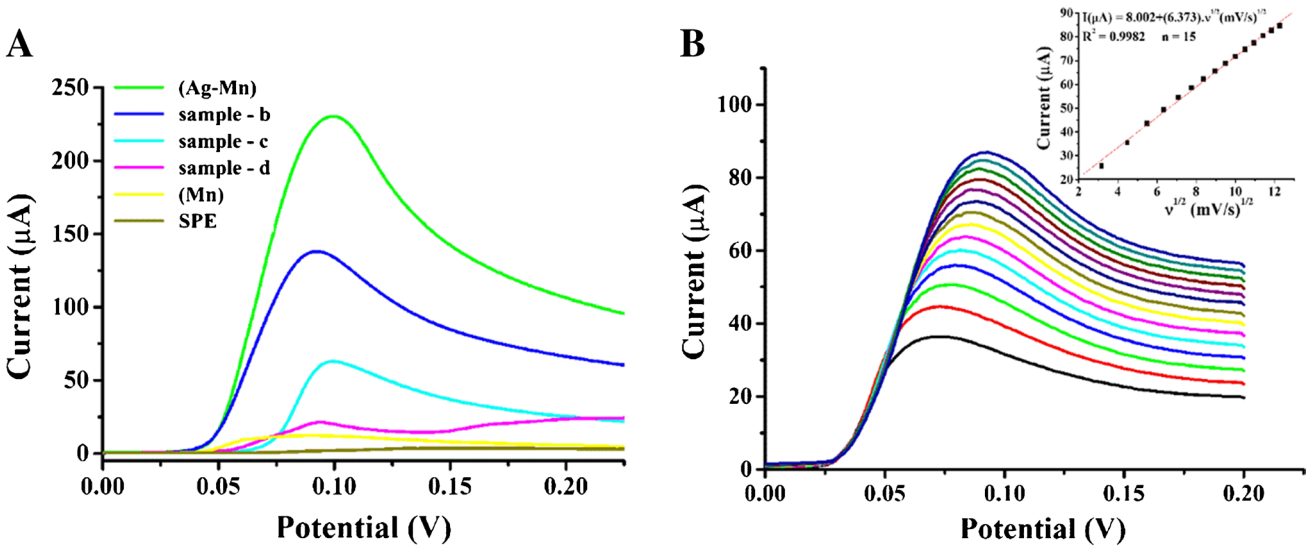

Fig. 2 **A** Voltammetric peaks of different electrodes in 0.1 M $NaNO_3$ for 100 mM NaCl at a scan rate of 50 mV s^{-1} (**B**) Voltammetric peaks of Ag-Mn/SPE in 0.1 M $NaNO_3$ with 5 mM NaCl at different scan rates (10–150 mV s^{-1}) and a potential window of 0 to + 0.2 V (vs. Ag/AgCl)

beyond doubt, proves that silver in the electrode material reacts with chloride ions and forms silver chloride.

Estimation of chloride ions

The differential pulse voltammetric (DPV) technique was used to quantitatively analyze chloride ions on the fabricated electrodes, to achieve more sensitivity and detection range. The electrodes were tested in 0.1 M sodium nitrate solution in a potential window of − 0.25 to + 0.25 V with an increment potential of 1 mV and pulse amplitude of 25 mV. Performing each test on individual (fresh) electrodes avoided the possibility of surface fouling. It is clear from the DPV curves obtained with different catalysts that the peak current increases with the concentration of chloride ions (Fig. 3A). It is also observed that the magnitude of peak current is proportional to the chloride concentration up to 52 mM, which is the dynamic range. The linear range of the sensor was determined to be 40 mM (Table S4, Fig. S6). Figure 3A inset shows the calibration curve between the peak current and chloride ion concentration. The corresponding regression equation containing slope and intercept along with their uncertainty is expressed as $I\ (\mu A) = (-0.24 \pm 0.46) + (0.72 \pm 0.02) \times C\ (mM)$ with a regression coefficient of 0.9943. The working area of the electrode is 3.142×10^{-2} cm^2 ($r = 0.1$ cm) and sensitivity is calculated to be 22.93 ± 0.64 µA mM^{-1} cm^{-2}. The limit of detection (LOD) for the proposed sensor is calculated to be 207 ± 7 µM.

Analytical performance of the sensor

The fabricated sensor was tested for its reproducibility to determine the feasibility in real-time applications. The voltammetric current response for 40 mM NaCl was measured on ten different electrodes. The relative standard deviation was 2.38%, indicating good reproducibility and further supporting the applicability of the sensor strips. The fabricated sensor was also tested for the interference of commonly found species in sweat, with concentration on the higher end of the normal range. Figure 3B shows the electrochemical response of the sensor to 200 mM sodium chloride and potassium chloride, 25 mM potassium nitrate, 50 mM urea, 0.10 mM uric acid, 0.10 mM Glucose, 0.10 mM dopamine hydrochloride, 0.10 mM ascorbic acid, 0.42 mM sodium acetate, 1.10 mM sodium phosphate, 2 mM sodium sulphate, 5 mM EDTA, 95 µM sodium fluoride, 6.3 µM potassium bromide, 75 µM potassium iodide, 20 mM sodium bicarbonate, 100 µM sodium sulphide, and 250 µM sodium hydroxide. From the figure, it is obvious that the sensor did not produce any significant current response to species other than chloride ions. The highly selective nature of the developed sensor proves the potential for real-time applications.

Fabrication of biosensor strip for PoCT applications

A chloride biosensor strip was fabricated by optimizing each component, as mentioned in the "Fabrication of a biosensor test strip" section, ultimately aimed at PoCT applications. The size of the spacer and adhesive layers was determined with reference to the base layer, SPE. The electrolyte

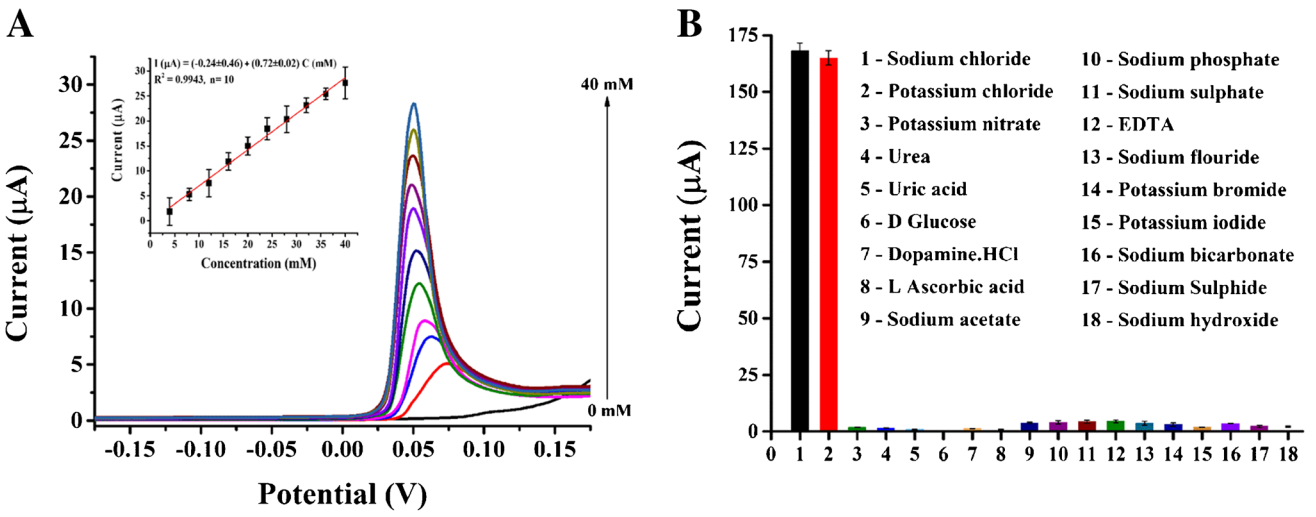

Fig. 3 **A** DPV of Ag-Mn/SPE for different concentrations of NaCl tested in 0.1 M $NaNO_3$ at a potential window of − 0.25 to + 0.25 V (vs. Ag/AgCl) Inset: Calibration plot of peak current vs. NaCl concentration. **B** Voltammetric peak current obtained on the Ag-Mn/SPE for chloride and other interfering species tested in 0.1 M $NaNO_3$ at a potential window of − 0.25 to + 0.25 V (vs. Ag/AgCl)

layer was made up of a cellulose membrane treated with sodium nitrate. Figure 4A shows the plot of peak current recorded for 20 mM chloride solution using the cellulose membrane treated with different concentrations of sodium nitrate. Among different concentrations, 2 M sodium nitrate incorporated membrane showed good reproducibility and peak current. No marked increase in current response was observed above this concentration. So, the biosensor strip was fabricated using a 2 M sodium nitrate incorporated membrane for further studies. They were tested with a simulated sweat solution to check the real-time application of the fabricated strip.

Different concentration of sodium chloride solution was prepared in simulated sweat solution. 20 µL of the test solution was introduced at the front end of the strip. The sample travels through the electrolyte membrane and gets collected in the working area guided by the designs made in the spacer layer. Figure 4B shows the electrocatalytic detection of chloride of different concentrations performed using DPV. The well-defined peaks in the voltammogram show the excellent selectivity of the fabricated sensor towards chloride ions, even in the presence of several electrolytes, amino acids, carbohydrates, nitrogenous substances, and vitamins commonly found in sweat. Figure 4C and D demonstrates the logarithmic increase in peak current with increasing chloride concentration over two detection ranges, i.e., a first detection range from 0.1 to 5 mM (Fig. 4C) and a second detection range from 5 to 200 mM (Fig. 4D) concentration of NaCl, respectively.

The borderline of CF diagnosis is 40–59 mM for adults and 30–59 mM for children. Chloride concentration in CF-positive adults can be as high as 150 mM. The wide detection range enables the fabricated sensor to test samples from individuals with negative, borderline, and positive ranges of chloride levels without any dilution or preprocessing. The corresponding regression equation for Fig. 4C is expressed with uncertainty as $I\ (\mu A) = (18.87 \pm 0.47) + (7.81 \pm 0.79) \times \log C(mM)$ with a regression coefficient of 0.9612. The regression equation for Fig. 4D is expressed as $I\ (\mu A) = (-5\,1.65 \pm 2.17) + (94.54 \pm 1.94) \times \log C(mM)$ with a regression coefficient of 0.9954. The sensitivity of the fabricated sensor is calculated from the regression equations as 250 ± 25 µA $(\log mM)^{-1}\ cm^{-2}$ for Fig. 4C, and 3010 ± 60 µA $(\log mM)^{-1}\ cm^{-2}$ for Fig. 4D. The lower detection limit is calculated from Fig. 4C as 17 ± 6 µM.

The complete prototype of the biosensor test strip was fabricated using the electrocatalyst-printed screen-printed electrode and electrolyte-incorporated membrane. It does not require any sample preparation steps, and the sweat sample can be placed directly for analysis (details of the testing

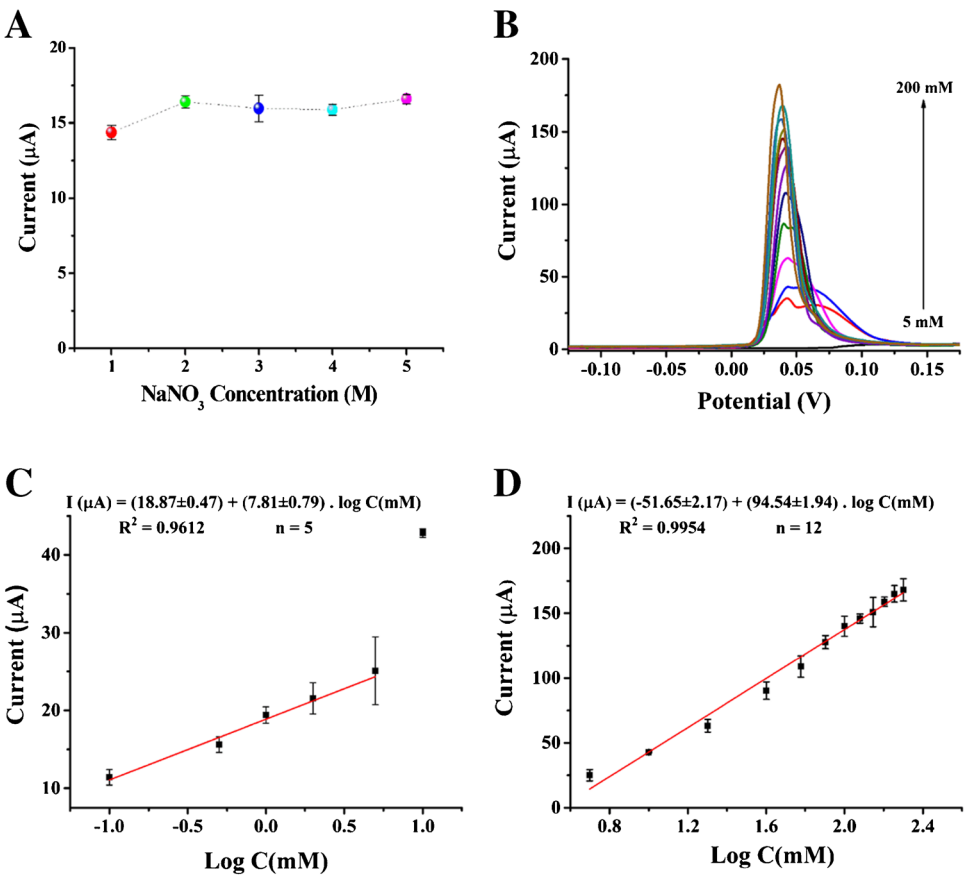

Fig. 4 **A** Peak current of the strip fabricated with different electrolyte concentrations in the membrane. **B** DPV of test strip tested in simulated sweat solutions with 0, 5, 10, 20, 40, 60, 80, 100, 120, 140, 160, 180, and 200 mM chloride. **C** Calibration plot for strip tested in simulated sweat with 0.1–5 mM chloride ion concentration. **D** Calibration plot for strip tested in simulated sweat with 5–200 mM chloride 0.1–5 mM chloride ion concentration

procedures are presented in Section S2). Thus an affordable, disposable, highly selective, and sensitive monitoring of chloride ions is made possible. The developed sensor was compared with similar biosensors reported in the literature (Table S5). There are reports based on the screen-printed electrode, but most have not been fabricated as disposable test strips. On the contrary, some reports show very low detection limits, but they are fabricated using standard laboratory electrodes such as glassy carbon electrodes and hence cannot be translated into POC test strips. In comparison, the completely fabricated sensor strip reported in this work can detect negative, borderline, and positive cases of CF with a good lower detection limit. The main advantages of the developed sensor test strip include a wide linear range in the human sweat.

Real sample analysis

Sweat samples were collected from a healthy individual during a treadmill run and analyzed to test the fabricated biosensor strips in real-time. The regression equation from Fig. 4B inset is used to estimate chloride ions, as simulated sweat solution ("Real sample analysis" section) was used. The collected sweat samples were tested in a clinical laboratory using the instrument Alinity ci-series, Abbot, which works with ion selective electrodes (ISE). Then, a known concentration of chloride was added to the sweat sample and used to estimate the chloride level by fabricated sensor strips. The difference in chloride levels estimated by laboratory testing and the fabricated sensor is shown in Table 1. All the tested samples show less than 10% error compared with values obtained from the clinical laboratory.

Conclusion

An electrochemical chloride sensor using silver-manganese nanocomposite was successfully fabricated by screen-printing and shown to have a wide linear range, good selectivity, and sensitivity. Morphological studies of the catalyst revealed the presence of close-packed nanorods of quasi-prism-like structure. The crystallographic studies revealed that the synthesized nanocomposite was in a tetragonal arrangement. The biosensor strip was fabricated with an electrolyte membrane and tested with collected sweat samples, which detected negative, borderline, and positive chloride concentration levels in sweat for CF diagnosis. The estimated chloride concentration was in good agreement with clinical lab tests. The results obtained are promising for real-time detection of chloride ions and diagnosis of cystic fibrosis.

Table 1 Real sample analysis of the fabricated sensor strip

Sample	Clinically tested concentration (mM)	Estimated concentration (mM)	Error %
1	47.9	52.29 ± 2.05	9.16
2	97.9	105.43 ± 2.36	7.69
3	147.9	150.08 ± 2.96	1.47
4	191.4	180.6 ± 0.62	5.64

Supplementary Information The online version contains supplementary material available at https://doi.org/10.1007/s00604-022-05431-1.

Acknowledgements Arun Kumar P expresses his sincere thanks to COE-AMGT, Amrita Vishwa Vidyapeetham for diffraction and thermal analysis; SITRA, Coimbatore for HRSEM analysis; sophisticated test and instrumentation centre, and CUSAT for HRTEM analysis.

Funding The authors acknowledge that the Department of Science & Technology, Government of India [SP/YO/692/2018 dated 28/09/2018] and Department for Biotechnology, Ministry of Science and Technology, Government of India [102/IFD/SAN/1555/2018–2019 dated 13/08/2018] supported this work.

Declarations

Ethics approval and consent to participate All procedures performed in the study involving human participants were in accordance with the ethical guidelines of the institute. This work does not contain any studies with animals. Informed consent was obtained from all the individuals included in the study.

Conflict of interest The authors declare no competing interests.

References

1. Davies JC, Alton EWFW, Bush A (2007) Cystic fibrosis. Br Med J 335:1255–1259. https://doi.org/10.1136/bmj.39391.713229.AD
2. VanDevanter DR, Kahle JS, O'Sullivan AK et al (2016) Cystic fibrosis in young children: a review of disease manifestation, progression, and response to early treatment. J Cyst Fibros 15:147–157. https://doi.org/10.1016/j.jcf.2015.09.008
3. Gonzalo-Ruiz J, Mas R, de Haro C et al (2009) Early determination of cystic fibrosis by electrochemical chloride quantification in sweat. Biosens Bioelectron 24:1788–1791. https://doi.org/10.1016/j.bios.2008.07.051
4. Trnkova L, Adam V, Hubalek J et al (2008) Amperometric sensor for detection of chloride ions. Sensors 8:5619–5636. https://doi.org/10.3390/s8095619
5. Toh HS, Batchelor-Mcauley C, Tschulik K, Compton RG (2013) Electrochemical detection of chloride levels in sweat using silver nanoparticles: a basis for the preliminary screening for cystic fibrosis. Analyst 138:4292–4297. https://doi.org/10.1039/c3an00843f
6. Bujes-Garrido J, Arcos-Martínez MJ (2016) Disposable sensor for electrochemical determination of chloride ions. Talanta 155:153–157. https://doi.org/10.1016/j.talanta.2016.04.038

7. Bujes-Garrido J, Izquierdo-Bote D, Heras A et al (2018) Determination of halides using Ag nanoparticles-modified disposable electrodes. A first approach to a wearable sensor for quantification of chloride ions. Anal Chim Acta 1012:42–48. https://doi.org/10.1016/j.aca.2018.01.063
8. Kwak B, Park S, Lee HS et al (2019) Improved chloride ion sensing performance of flexible Ag-NPs/AgCl electrode sensor using Cu-BTC as an effective adsorption layer. Front Chem 7:637. https://doi.org/10.3389/fchem.2019.00637
9. Chou JC, Tseng TW, Liao YH et al (2019) Analysis of chloride ion sensor modified by graphene oxide under microfluid flow. IEEE Sens J 19:3217–3223. https://doi.org/10.1109/JSEN.2019.2892041
10. Cunha-Silva H, Julia Arcos-Martinez M (2019) Development of a selective chloride sensing platform using a screen-printed platinum electrode. Talanta 195:771–777. https://doi.org/10.1016/j.talanta.2018.12.008
11. Álvarez-Romero GA, Ramírez-Silva MT, Galán-Vidal CA et al (2010) Development of a chloride ion-selective solid state sensor based on doped polypyrrole-graphite-epoxy composite. Electroanalysis 22:1650–1654. https://doi.org/10.1002/elan.200900601
12. Fan L, Xu T, Feng J et al (2020) Tripodal squaramide derivative as a neutral chloride ionophore for whole blood and sweat chloride measurement. Electroanalysis 32:805–811. https://doi.org/10.1002/elan.201900693
13. Zhang M, Wang C, Zhang Z et al (2019) A novel carbon paste electrode for sensitive, selective and rapid electrochemical determination of chloride ion based on three-dimensional graphene. Sens Actuators, B Chem 299:126951. https://doi.org/10.1016/j.snb.2019.126951
14. Song KS, Sakai T, Kanazawa H et al (2003) Cl- sensitive biosensor used electrolyte-solution-gate diamond FETs. Biosens Bioelectron 19:137–140. https://doi.org/10.1016/S0956-5663(03)00174-X
15. Hung SC, Wang YL, Hicks B et al (2008) Detection of chloride ions using an integrated AgAgCl electrode with AlGaNGaN high electron mobility transistors. Appl Phys Lett 92:2012–2015. https://doi.org/10.1063/1.2927372
16. Abbas Y, Olthuis W, Van Den Berg A (2013) A chronopotentiometric approach for measuring chloride ion concentration. Sens Actuators, B Chem 188:433–439. https://doi.org/10.1016/j.snb.2013.07.046
17. Huang JF (2009) Silver UPD ultra-thin film modified nanoporous gold electrode with applications in the electrochemical detection of chloride. Talanta 77:1694–1700. https://doi.org/10.1016/j.talanta.2008.10.005
18. Harris N, Cranny A, Rivers M, Smettem K (2015) Applications of a wireless chloride sensor in environmental monitoring. SAS 2015 - 2015 IEEE Sensors Appl Symp Proc p. 1–5. https://doi.org/10.1109/SAS.2015.7133591
19. Bin Q, Wang M, Wang L (2020) Ag nanoparticles decorated into metal-organic framework (Ag NPs/ZIF-8) for electrochemical sensing of chloride ion. Nanotechnology 31:125601. https://doi.org/10.1088/1361-6528/ab5cde
20. Rahman MM, Khan SB, Gruner G et al (2013) Chloride ion sensors based on low-dimensional α-MnO_2-Co_3O_4 nanoparticles fabricated glassy carbon electrodes by simple I-V technique. Electrochim Acta 103:143–150. https://doi.org/10.1016/j.electacta.2013.04.067
21. Sohal N, Maity B, Shetti NP, Basu S (2021) Biosensors based on MnO_2Nanostructures: a review. ACS Appl Nano Mater 4:2285–2302. https://doi.org/10.1021/acsanm.0c03380
22. Lazanas AC, Prodromidis MI (2021) Two-dimensional inorganic nanosheets: production and utility in the development of novel electrochemical (bio)sensors and gas-sensing applications. Microchim Acta 188:6. https://doi.org/10.1007/s00604-020-04674-0
23. Rojas D, Hernández-Rodríguez JF, Della Pelle F et al (2022) New trends in enzyme-free electrochemical sensing of ROS/RNS. Application to live cell analysis. Microchim Acta 189:102. https://doi.org/10.1007/s00604-022-05185-w
24. Ak P, Suneesh PV, NairSB GBKTG (2021) Complete fabrication of a nonenzymatic glucose sensor with a wide linear range for the direct testing of blood samples. Electrochim Acta 395:139145. https://doi.org/10.1016/j.electacta.2021.139145
25. Sopstad S, Imenes K, Johannessen EA (2020) Chloride and pH determination on a wireless, flexible electrochemical sensor platform. IEEE Sens J 20:599–609. https://doi.org/10.1109/JSEN.2019.2944407
26. Xu G, Cheng C, Yuan W et al (2019) Smartphone-based battery-free and flexible electrochemical patch for calcium and chloride ions detections in biofluids. Sens Actuators, B Chem 297:126743. https://doi.org/10.1016/j.snb.2019.126743
27. Lynch A, Diamond D, Leader M (2000) Point-of-need diagnosis of cystic fibrosis using a potentiometric ion-selective electrode array. Analyst 125:2264–2267. https://doi.org/10.1039/b006379g
28. Choi D, Thaxton A, Kim K et al (2018) Sweat test for cystic fi brosis : wearable sweat sensor vs. standard laboratory test ☆. J Cyst Fibros 17:e35–e38. https://doi.org/10.1016/j.jcf.2018.03.005
29. Cinti S, Fiore L, Massoud R et al (2018) Low-cost and reagent-free paper-based device to detect chloride ions in serum and sweat. Talanta 179:186–192. https://doi.org/10.1016/j.talanta.2017.10.030
30. Kumar PA, Stanley J, Babu TGS, Suneesh PV (2018) Synthesis of nickel-aluminium layered double hydroxide and its application in non-enzymatic glucose sensing. Mater Today Proc 5:16125–16131. https://doi.org/10.1016/j.matpr.2018.05.098
31. Sun M, Lan B, Lin T et al (2013) Controlled synthesis of nanostructured manganese oxide: crystalline evolution and catalytic activities. CrystEngComm 15:7010–7018. https://doi.org/10.1039/c3ce40603b